Reply to Referee #2

We would like to thank the Referee for their positive and constructive report. We are glad our revised manuscript is considered worth publication in SciPost Physics. We also thank the Referee for their new suggestions which we implemented in the new submitted version of our manuscript. We answer in the following to all the points they raised.

Report: **The updated manuscript has been significantly expanded, and now presents a much more general methodology for determining vortex dynamics and energetics in complex geometries. As such, I think the revised manuscript does open pathways for new research, and therefore satisfies the criteria for publication in SciPost Physics.**
I have a few minor comments regarding the revisions, but once these have been addressed, I recommend the manuscript be accepted for publication.

Requested changes **The authors have addressed almost all my previous comments satsifactorily, although I have responses to some minor aspects of the first two points:**

- **The Jacobi theta function may be straightforward to calculate numerically, but mathematically it requires an infinite series to be defined, whereas** $\sin(x)$ **can be defined in terms of elementary operations (eg. as a ratio of two sides of a triangle, or via complex exponentiation). Since the theta function involves an infinite number of operations, I do not think it can strictly be referred to as "closed-form". Regardless, I leave the terminology up to the authors.**

We understand the Referee's concern about the suitability of the term "closed-form", for this reason we have decided to adopt a different terminology. We have slightly expanded paragraph 9 of the Introduction to highlight the novelty of our results with respect to those derived in previous works as infinite series. The term "closed-form" has been replaced in the remainder of the manuscript, as well (final paragraph of the Introduction and last sentence of Sec. 5.1).

- **A number of improvements have been made to the wording around the fluid compressibility in the introduction, but the second sentence still refers to superfluids having "negligible compressibility", which is not true for ultracold atomic gases (as I pointed out in my previous report). I suggest removing this.**

We are glad the Referee appreciated our revisions and we agree that "negligible compressibility" is not as general of a property of superfluids as the absence of viscosity and dissipation. We have thus removed it, complying with the Referee's suggestion.

I also have a few minor comments regarding the new material:

- **Could the title be made more general? The emphasis of the revised manuscript seems to be more on the general method, rather than on the specific case of an elliptical geometry, but this is not reflected in the title.**

We would like to thank the Referee for suggesting a revision of the title. Indeed, we have modified it to "Conformal maps and superfluid vortex dynamics on curved and bounded surfaces: the case of an elliptical boundary" and we believe that it now better reflects the new contribution of our work.

- **Paragraph 2 of the introduction reads: "Vortices in two-dimensional films have simpler dynamics...". This seems to be implying that the dynamics are simpler than in three-dimensional systems, but the preceding text does not mention three-dimensional systems specifically, so the word "simpler" appears out of place. I suggest altering this wording slightly.**

We rephrased paragraph 2 of the Introduction adding a sentence about the general framework of vortices in three-dimensional systems. In our opinion, this removes the ambiguity around the word "simpler" referred to two-dimensional configurations, thus improving the readability of the manuscript.

- **The sentence directly after this reads: "Hence a point-vortex model applies". This does not immediately follow from the dynamics being restricted to 2D. A point-vortex approximation also requires core sizes to be small compared to other relevant lengthscales (eg. the system size, distances to other vortices). I think this is worth mentioning here.**

We totally agree that such a separation of different length scales underlies the point-vortex approximation and is definitely worth mentioning. We did that in the revised version of our manuscript.

- **Paragraph 4 begins: "Most cold atom experimental platforms are able to produce essentially uniform systems". I am not sure if "most" is true, so I suggest weakening this claim to eg. "many".**

We changed the wording, following Referee's suggestion.

- **The acronym "BEC" is defined twice in the introduction.**

We have fixed the second definition, using directly the acronym.

- **In paragraph 8 of the introduction, the authors refer to "the vortex interpretation of the boundary-value problem". I am not sure what this means. Can the authors clarify this sentence?**

With that sentence we refer to the well-known equivalence between superfluid vortices on a planar geometry and a two-dimensional Coulomb gas of electric charges. Nonetheless, we rephrased the whole paragraph in order to clarify the similarities between the two systems, as well as to put emphasis on the additional features of vortex dynamics.

- **Regarding Eq (10), it would be helpful to specify that * denotes complex conjugation.**

We have specified the notation below Eq. (10).

- **I was confused by the definitions of n_0 and n_i, introduced in Sec 3.1:**

  i) **Following Eq (20), n_0 is described as the "quantized circulation around the boundary", although it is not clear exactly which boundary is being referred to. Shortly afterwards, following Eq (23), $n_i = n_0 - 1$ is described as "the circulation quantum around the circular boundary at R". So are n_i and n_0 defined around different boundaries? My best guess is that n_0 is the winding around the w-plane (elliptical) boundary, while n_i is the winding around the z-plane (circular) boundary, but this appears to be reversed in the caption of Fig 1. I suggest the authors clarify this.**

  ii) **Is the difference of -1 between the two winding numbers n_i and n_0 related to the pole at the origin of the z-plane? It would be useful to specify where this difference comes from.**

We understand Referee's confusion and rewrote the discussion of $\mathfrak{n}_0$ and $\mathfrak{n}_1$. On the one hand, $\mathfrak{n}_0$ corresponds to the charge of the additional vortex located at the centre of the disk when studying a single vortex outside the circular boundary. On the other hand, $\mathfrak{n}_i$ is properly defined as "the circulation quantum around the circular boundary at R". For instance, the simple case of a single vortex outside a circular boundary requires a negative image inside the boundary, which is indeed responsible for the -1 appearing in the relation between the two winding numbers $\mathfrak{n}_i = \mathfrak{n}_0 - 1$. Ultimately, one chooses $\mathfrak{n}_0$ in order to fix the value of the circulation $\mathfrak{n}_i$ along the boundary.

We split the discussion in Sec. 3.1 into two parts, one for a vortex inside and one for a vortex outside a circular boundary. We believe the circulation quanta $\mathfrak{n}_0$ and $\mathfrak{n}_i$ are now properly specified and easier to grasp.

- **Following Eq (29), the authors point out that for small distances $d \ll a$ from the ellipse, the energy diverges as $\log(2d)$. Is this easy to see from Eq (29)? Which terms contribute or drop out in this limit?**

A simple understanding comes from the fact that if the vortex is very close to the boundary, the latter looks locally flat. In this case, the image vortex is at a distance d behind the boundary to satisfy the condition of tangential flow, giving a net separation $2d$ between the vortex and its image. Recalling the standard results for a vortex dipole on the plane, the energy and the tangential velocity then vary like $\ln(2d)$ and $1/(2d)$, respectively. We agree that the discussion was not very clear, therefore we expanded it with more details below Eq. (30) in the revised version of our manuscript.

- **It would be useful to include color bars in the figures with color scale data, or at least a description of the color scale in the caption (eg. for Fig 2, blue $\rightarrow$ low energy, orange $\rightarrow$ high energy).**

We thank the Referee for this suggestion that improves the readability of the figures. We added a description of colour coding in the captions of Figs. 2, 5 and 8.

~~Superfluid vortex dynamics with an elliptical boundary~~ Conformal maps and superfluid vortex dynamics on curved and bounded surfaces: the case of an elliptical boundary

Matteo Caldara[1,⋆], Andrea Richaud[2], Pietro Massignan[2,†] and Alexander L. Fetter [3]

1 Scuola Internazionale Superiore di Studi Avanzati (SISSA), Via Bonomea 265, I-34136, Trieste, Italy

2 Departament de Física, Universitat Politècnica de Catalunya, Campus Nord B4-B5, E-08034 Barcelona, Spain

3 Department of Physics and Department of Applied Physics, Stanford University, Stanford, California 94305-4045, USA

⋆ mcaldara@sissa.it, † pietro.massignan@upc.edu

July 18, 2024

Abstract

Recent advances in cold-atom platforms have made real-time dynamics accessible, renewing interest in the motion of superfluid vortices in two-dimensional domains. Here we show that the energy and the trajectories of arbitrary vortex configurations may be computed on a complicated (curved or bounded) surface, provided that one knows a conformal map that links the latter to a simpler domain (like the full plane, or a circular boundary). We also prove that Hamilton's equations based on the vortex energy agree with the complex dynamical equations for the vortex dynamics, demonstrating that the vortex trajectories are constant-energy curves. We use these ideas to study the dynamics of vortices in a two-dimensional incompressible superfluid with an elliptical boundary, and we derive an analytical expression for the complex potential describing the hydrodynamic flow throughout the fluid. For a vortex inside an elliptical boundary, the orbits are nearly self-similar ellipses.

Contents

1 Introduction

Quantized vortices are fundamental topological excitations of superfluids, such as liquid ^{4}He-II [1], dilute one- and two-component Bose-Einstein condensates (BECs), and two-component fermionic mixtures [2,3]. At low temperatures, these systems become nearly ideal fluids with negligible ~~compressibility,~~ viscosity~~,~~ and dissipation. As a result, superfluid vortices obey the dynamical equations of classical hydrodynamics [4,5] augmented with the condition of quantized vorticity [6,7].

~~Vortices in thin two-dimensional films have simpler dynamics because bending modes freeze out.~~ Three-dimensional vortex lines have various bending modes that complicate the analysis of their dynamics. The situation becomes much simpler in two dimensions because only translational motion remains. In addition, for dilute-gas BECs, the typical diameter of the vortex cores is much less than all other length scales like the trap size or intervortex separation. Hence ~~a point-vortex model applies~~ these vortices act like point vortices, with the x and y coordinates as canonically conjugate variables and first-order equations of motion.

In the 1960s, experiments with rotating superfluid He-II [8,9] stimulated theoretical studies of equilibrium two-dimensional (2D) vortex states in cylinders [10] and annuli [11]. More recently, some of us have studied the dynamics of quantized vortices on nonplanar 2D surfaces [12–15] relying on a complex potential that exploits the properties of conformal transformations.

It is useful to describe a superfluid system at low temperature with a macroscopic condensate wave function $\Psi(\boldsymbol{r}) = \sqrt{n(\boldsymbol{r})}e^{i\Phi(\boldsymbol{r})}$ in terms of two real fields, the number density $n(\boldsymbol{r})$ and the phase $\Phi(\boldsymbol{r})$. The latter determines the two-dimensional superfluid velocity through $\boldsymbol{v} = \hbar\boldsymbol{\nabla}\Phi/M$, with M the atomic mass. The flow is then irrotational $\boldsymbol{\nabla}\times\boldsymbol{v} = 0$ everywhere except at the phase singularities associated with the vortex cores.

~~Most~~ Many cold-atom experimental platforms are able to produce essentially uniform systems [16,17], with negligible local changes of the density in the bulk of the superfluid. In the absence of sound waves from acoustic excitations, the continuity equation for particle conser-

vation, $\partial_t n + \boldsymbol{\nabla}\cdot(n\boldsymbol{v}) = 0$, implies that the flow is effectively incompressible, with $\boldsymbol{\nabla}\cdot\boldsymbol{v} = 0$. As a consequence, such a two-dimensional flow may also be described by the stream function $\chi(\boldsymbol{r})$, in terms of which the superfluid velocity in the xy plane becomes $\boldsymbol{v} = (\hbar/M)\hat{\boldsymbol{z}}\times\boldsymbol{\nabla}\chi$.

We now have two distinct representations of the hydrodynamic velocity $\boldsymbol{v}$. When written out in detail, the cartesian components of $\boldsymbol{v}$ satisfy the Cauchy-Riemann equations. Hence χ and Φ can be interpreted as the real and imaginary parts of an analytic function of a complex variable $z = x + iy$. In this way, we construct the complex potential defined as

$$F(z) = \chi(\boldsymbol{r}) + i\Phi(\boldsymbol{r}), \tag{1}$$

with $\boldsymbol{r}$ the two-dimensional position vector. The Cauchy-Riemann conditions give the following compact representation of the hydrodynamic flow velocity:

$$v_y + iv_x = \frac{\hbar}{M}\frac{dF(z)}{dz}. \tag{2}$$

Early experiments on rotating ^{4}He-II used circular containers with rotationally invariant walls. For such a geometry, surface roughness at the wall triggers the nucleation of vortices, which then migrate into the bulk of the superfluid. In contrast, a rotating elliptical boundary pushes the superfluid, imparting angular momentum even though the flow remains irrotational for slow rotations. As the rotation rate increases, however, isolated vortices eventually appear within the container [18]. These predictions found a solid confirmation in experimental studies of vortex states in rotating superfluid ^{4}He-II for three elliptical containers with different eccentricities [19].

Reference [18] focused on the energy and angular momentum of a vortex in an elliptical boundary, with no consideration of the associated vortex dynamics, which was experimentally inaccessible at that time. More recently, the creation of cold-atom ~~Bose-Einstein condensates (~~BECs~~)~~ has allowed direct real-time studies of vortex dynamics [20–22]. In this context, we study here the motion of two-dimensional superfluid vortices outside and inside a stationary elliptical boundary. An additional motivation is the recent experimental accessibility of such configurations using digital micromirror devices (DMDs) [17, 23–27].

Previous studies of vortices [18] or two-dimensional point charges [28] with elliptical boundaries have used standard methods of mathematical physics with elliptic coordinates [29], leading to real solutions expressed as infinite series whose convergence requires detailed analysis. Here, instead, we rely on complex variables and conformal ~~transformations~~ maps to solve the same problems, giving ~~closed-form~~ explicit solutions expressed in terms of ~~standard~~ well-known functions of mathematical physics.

~~The vortex interpretation of the boundary-value problem yields more general results, for it also describes the vortex dynamics. In addition, the complex formalism gives not only the stream function χ (analogous to the lines of constant electrostatic potential) but also the vortex phase pattern Φ (analogous to the electric field lines).~~ The recent study [28] of two-dimensional point charges outside and inside an elliptical boundary obtained infinite series for the electrostatic potential and focused on finding equivalent sets of charged images. The similar problem of point vortices with the same geometry is far richer. In addition to determining the stream function χ for the vortices (analogous to the electrostatic potential for the charges), the dynamics of the vortices is also of great interest, particularly because of experiments with dilute-gas BECs. In addition, our complex formalism also gives the phase pattern Φ of the vortices (analogous to the electric field lines).

Reference [30] used a conformal transformation to relate the energy of a vortex on a curved surface to the corresponding energy on a simpler surface through the metric properties of the conformal map relating the two surfaces. Section 2 reviews and extends this technique to obtain the complex dynamics of a single vortex inside a general closed boundary in terms of

the complex dynamics in the simpler geometry. We also show that these dynamical equations agree with the real Hamilton's equations based on the energy as a function of the coordinates of the vortex. In Sec. 3, we study a single vortex both inside and outside a circular boundary, which serves as our simple geometry. Section 4 presents the Joukowsky transformation and its analytic properties that play an important role in our analysis. In Sec. 5 we study a single superfluid vortex outside a two-dimensional elliptical boundary. In the subsequent Sec. 6 we solve the more intricate problem of a single vortex in an elliptical domain. We obtain ~~a closed~~ an explicit analytical expression for the complex potential, leading to the equations of motion for a vortex inside an elliptical boundary. Their numerical solution gives the vortex trajectories, which are approximately but not exactly elliptical. We also generalize to a multivortex configuration, showing results for a symmetric vortex dipole. Finally, in Sec. 7, we summarize and suggest possible future extensions of our work. Appendix A presents an alternative (but equivalent) treatment of a vortex inside an ellipse, based on a direct transformation from a circle to the ellipse.

2 Conformal maps and basic physical properties

We here study the behaviour of a single positive quantized vortex either inside or outside a quite general curved boundary. It is convenient to solve this problem with a conformal map from a simpler standard boundary (for example a circle) to the general boundary (for example an ellipse). Let z be the complex plane with the standard boundary and w be the complex plane with the general boundary. Assume that $w(z)$ is the conformal map from the standard boundary to the general boundary, with inverse $z(w)$. Infinitesimal displacements on the two surfaces are related by

$$dz = e^{\sigma(w)} dw, \tag{3}$$

which defines the space-dependent complex scale factor

$$\frac{dz(w)}{dw} = z'(w) = e^{\sigma(w)} \quad \text{or, equivalently,} \quad \sigma(w) = \ln\big(z'(w)\big). \tag{4}$$

Reference [30] studies a real infinitesimal displacement with a real scale factor $e^{\omega(w)}$. They are essentially the same, with $\omega(w) = \mathrm{Re}\,\sigma(w)$. In the z plane, a vortex at z_0 has the complex potential $F_z(z; z_0)$ that is known explicitly. The corresponding complex potential for the general boundary in the w plane is

$$F_w(w; w_0) = F_z[z(w); z(w_0)]. \tag{5}$$

2.1 Energy of a single vortex

Since the energy $E_z = \frac{1}{2} nM \int d^2r\, |\boldsymbol{v}|^2$ in the z plane is purely kinetic, it is simple to find E_z of a single vortex using the stream function $\chi = \mathrm{Re}\, F_z(z; z_0)$ and the relation for the flow velocity $\boldsymbol{v} = (\hbar/M)\hat{\boldsymbol{n}} \times \boldsymbol{\nabla}\chi$, where $\hat{\boldsymbol{n}}$ is the unit normal to the z plane. Specifically, $E_z = \frac{1}{2}\hbar n \int d^2r\, \boldsymbol{v} \cdot \hat{\boldsymbol{n}} \times \boldsymbol{\nabla}\chi$. Some vector manipulations lead to

$$E_z = \frac{\hbar n}{2} \int d^2r\, [-\boldsymbol{\nabla} \cdot (\chi \hat{\boldsymbol{n}} \times \boldsymbol{v}) - \chi \hat{\boldsymbol{n}} \cdot (\boldsymbol{\nabla} \times \boldsymbol{v})] \tag{6}$$

In the first term, the divergence theorem gives integrals of the form $\oint d\boldsymbol{l} \cdot \boldsymbol{v}\chi$ around each boundary. The stream function on the j^{th} boundary takes the constant value χ_j and the remaining line integral is a positive or negative integer $\mathfrak{n}_j$ times $2\pi\hbar/M$, where the line

integral is in the positive sense and the sign of $\mathfrak{n}_j$ depends on the sense of the flow around the boundary.

The second term involves the vorticity $\boldsymbol{\nabla}\times\boldsymbol{v} = (2\pi\hbar\hat{\boldsymbol{n}}/M)\delta^{(2)}(\boldsymbol{r}-\boldsymbol{r}_0)$, centered at the vortex position, where the stream function diverges logarithmically. The integral thus reduces to a sum of two terms evaluated inside the vortex core (0-subscript):

$$\begin{aligned}\int d^2r\,\chi\,\hat{\boldsymbol{n}}\cdot(\boldsymbol{\nabla}\times\boldsymbol{v}) &= \int_0 d^2r\,\hat{\boldsymbol{n}}\cdot(\boldsymbol{\nabla}\times\boldsymbol{v})(\chi-\ln|\boldsymbol{r}-\boldsymbol{r}_0|)+\int_0 d^2r\,\hat{\boldsymbol{n}}\cdot(\boldsymbol{\nabla}\times\boldsymbol{v})\ln|\boldsymbol{r}-\boldsymbol{r}_0| \\ &= \frac{2\pi\hbar}{M}\lim_{\boldsymbol{r}\to\boldsymbol{r}_0}[\chi(\boldsymbol{r})-\ln|\boldsymbol{r}-\boldsymbol{r}_0|],\end{aligned} \tag{7}$$

where we assume that the vortex has a small hollow core excluding the vorticity at its center. A combination of these results gives

$$E_z = \frac{\pi\hbar^2 n}{M}\left(\sum_j \mathfrak{n}_j\chi_j - \tilde{\chi}_0^z\right), \tag{8}$$

where $\tilde{\chi}_0^z = \mathrm{Re}\lim_{z\to z_0}[F_z(z;z_0)-\ln(z-z_0)]$ is the regularized stream function. A completely analogous formula holds for the energy in the w plane $E_w = (\pi\hbar^2 n/M)\left(\sum_j \mathfrak{n}_j\chi_j - \tilde{\chi}_0^w\right)$.

Now consider the difference $E_w - E_z$. The conformal transformation conserves both the quantization integers $\mathfrak{n}_j$ and the circulation constants χ_j, so that

$$\begin{aligned}E_w - E_z &= \frac{\pi\hbar^2 n}{M}\left[\tilde{\chi}_0^z(z(w_0))-\tilde{\chi}_0^w(w_0)\right] \\ &= -\frac{\pi\hbar^2 n}{M}\mathrm{Re}\lim_{w\to w_0}\ln\left[\frac{z(w)-z(w_0)}{w-w_0}\right].\end{aligned}$$

The second line is obtained using the definitions of the regularized stream functions, together with the properties of the conformal map which ensure that the terms involving the full complex potential cancel. Writing $w = w_0+\delta$ and expanding $z(w)\approx z(w_0)+\delta\,z'(w_0)$ gives the very simple and general result

$$E_w = E_z - \frac{\pi\hbar^2 n}{M}\mathrm{Re}\,\sigma(w_0), \tag{9}$$

where $\sigma(w)$ is the scale factor defined in Eq. (4).

2.2 Dynamics of a single vortex

For a general complex potential $F(z)$, Eq. (2) gives the hydrodynamic velocity including the circulating flow around the vortex itself. This latter flow does not affect the vortex dynamics and must be subtracted off. In this way, the vortex in the z plane obeys the dynamical equation

$$i\dot{z}_0^* = \frac{\hbar}{M}\left[\frac{dF_z(z;z_0)}{dz}-\frac{1}{z-z_0}\right]_{z\to z_0}, \tag{10}$$

where * denotes complex conjugation. Similarly, the vortex at w_0 in the w plane has the dynamical equation

$$i\dot{w}_0^* = \frac{\hbar}{M}\left[\frac{dF_w(w;w_0)}{dw}-\frac{1}{w-w_0}\right]_{w\to w_0}. \tag{11}$$

Here, however, we have a conformal map $w(z)$ relating the two planes, so that the complex potential in the w plane becomes $F_w(w;w_0) = F_z[z(w);z(w_0)]$. As a result, we can write

$$\frac{dF_w(w;w_0)}{dw} = z'(w)\,\frac{dF_z(z(w);z(w_0))}{dz},$$

and

$$i\dot{w}_j^* = i\dot{z}_j^* e^{\sigma(w_j)} + \frac{\hbar c_j}{2M}\sigma'(w_j). \tag{18}$$

Reference [30] obtained our Eq. (17) in their Eq. (85), but the approach outlined above seems simpler and more direct. In contrast, our relation (18) for the vortex velocity is new, since Ref. [30] explicitly excluded vortex dynamics from its consideration. Interestingly, the contributions to the energy arising from the scale factors are independent of the sign of the vortices.

2.4 Example: conformal map from a plane to the surface of a cylinder

The conformal map $z_\pm(w) = e^{\pm iw}$ takes the flat z plane to the curved w surface of a cylinder with unit radius. We write $w = x + iy$ so that $z_\pm(w) = e^{\pm ix}\, e^{\mp y}$. This transformation is 2π periodic in x, which is the angular direction around the cylinder, while y becomes the axial direction along the length of the cylinder. Appendix A of Ref. [12] discusses this transformation in more detail. Here, we note that $z'_\pm(w_0) = e^{\sigma^\pm(w_0)} = \pm ie^{\pm iw_0}$, so that $\sigma^\pm(w_0) = \pm i\pi/2 \pm iw_0$.

Since a single vortex in an unbounded z plane remains stationary, the term $i\dot{z}_0^*$ in Eq. (13) vanishes, leaving the result $i\dot{w}_0^* = i\dot{x}_0 + \dot{y}_0 = \pm i\hbar/(2M)$. This means that the vortex precesses uniformly around the cylinder with quantized speed $\pm\hbar/(2M)$ in either direction at fixed height y_0, as found in Ref. [12] by a different method. This example is interesting because the motion of the vortex arises solely from the scale factor.

Similarly, the interaction energy of a vortex dipole at z_1 and z_2 on the z plane is $E_z = (2\pi\hbar^2 n/M)\,\mathrm{Re}\ln(z_1 - z_2)$. The interaction energy of a dipole with vortices at w_1 and w_2 on the surface of a cylinder is readily found using Eq. (17) to be

$$\begin{aligned} E_w &= \frac{2\pi\hbar^2 n}{M}\left\{\mathrm{Re}\ln[z_+(w_1) - z_+(w_2)] - \frac{1}{2}\mathrm{Re}\left[\sigma^+(w_1) + \sigma^+(w_2)\right]\right\} \\ &= \frac{2\pi\hbar^2 n}{M}\,\mathrm{Re}\ln\left[\sin\left(\frac{w_1 - w_2}{2}\right)\right] + \text{const.} \end{aligned} \tag{19}$$

This result coincides with the one found via a more complicated route in Eq. (27) of Ref. [12].

3 Single vortex with a circular boundary

We now apply this general formalism, with the z plane containing a circular boundary of radius R and the w plane containing an elliptical boundary. In this section, we review the elementary solutions for a single vortex at z_0 both inside and outside a circular boundary of radius R [5]. They rely on a single opposite-sign image vortex at $z'_0 = R^2/z_0^*$ on the opposite side of the circular boundary. The following section then describes the Joukowsky conformal transformation that maps concentric circles in the z plane to confocal ellipses in the w plane.

3.1 Vortex dynamics

As noted above, the complex potential for a vortex with a circular boundary involves a single opposite-sign image. We now present the two cases of a vortex inside/outside the circular boundary, which require an image vortex outside/inside the boundary.

3.1.1 Vortex inside circular boundary

The complex potential for a positive vortex on the z plane inside a circular boundary of radius R is

$$F_{\text{inside-circle}}(z; z_0) = \ln(z - z_0) - \ln\left(z - z'_0\right), \tag{20}$$

The first term of Eq. (20) describes circulating flow around the vortex and does not contribute to the vortex dynamics. As a result, only the second term is relevant and we have the complex dynamical equation

$$i\dot{z}_0^* = \frac{\hbar}{Mz_0}\frac{|z_0|^2}{R^2-|z_0|^2}. \tag{21}$$

For this interior vortex the uniform precession rate is

$$\dot{\theta}_0 = \frac{\hbar}{M(R^2-r_0^2)}. \tag{22}$$

3.1.2 Vortex outside circular boundary

The complex potential for a positive vortex on the z plane outside the circular boundary is

$$F_{\text{outside-circle}}(z;z_0) = \ln(z-z_0) - \ln\left(z-z_0'\right) + \mathfrak{n}_0 \ln z. \tag{23}$$

Here the last term represents an $\mathfrak{n}_0$-fold quantized circulation around the origin, where $\mathfrak{n}_0$ is a general integer. Note that the circulation $\mathfrak{n}_i$ around the circular boundary at radius R includes both the central vortex and the negative image at distance $R^2/r_0 < R$, giving $\mathfrak{n}_i = \mathfrak{n}_0 - 1$, using the general notation from Sec. 2.1. It is straightforward to find the precession rate for a vortex outside the circular boundary, that is

$$\dot{\theta}_0 = \frac{\hbar}{Mr_0^2}\left(\mathfrak{n}_0 - \frac{r_0^2}{r_0^2-R^2}\right) = \frac{\hbar}{Mr_0^2}\left(\mathfrak{n}_i - \frac{R^2}{r_0^2-R^2}\right). \tag{24}$$

This result reproduces Eq. (B8) in Ref. [12].

3.2 Energy of one vortex

We now use Eq. (8) to find the energy E_z of a single vortex with a circular boundary. Specifically, we need the stream function

$$\chi_{\text{circle}}(\boldsymbol{r};\boldsymbol{r}_0) = \text{Re}\, F_{\text{circle}}(z;z_0) = \mathfrak{n}_0 \ln r + \ln|\boldsymbol{r}-\boldsymbol{r}_0| - \ln|\boldsymbol{r}-\boldsymbol{r}_0'|, \tag{25}$$

with $\boldsymbol{r} = (r,\theta)$ in polar coordinates and similarly for $\boldsymbol{r}_0 = (r_0,\theta_0)$ and $\boldsymbol{r}_0' = (R^2/r_0,\theta_0)$.

For an exterior vortex, there are two boundaries: an outer circle at R_∞ where $\mathfrak{n}_{\text{out}} = \mathfrak{n}_0$ and $\chi_{\text{out}} = \mathfrak{n}_0 \ln R_\infty$; and an inner circle at R where $\mathfrak{n}_{\text{in}} = -\mathfrak{n}_0 + 1$ and $\chi_{\text{in}} = \mathfrak{n}_0 \ln R + \ln(r_0/R)$. In addition, we need $\tilde{\chi}_0^z = \mathfrak{n}_0 \ln r_0 - \ln|r_0 - R^2/r_0|$. Substitution into Eq. (8) gives the energy

$$E_{\text{circle}} = \frac{\pi\hbar^2 n}{M}\left[\mathfrak{n}_0^2 \ln\left(\frac{R_\infty}{R}\right) - 2\mathfrak{n}_0 \ln\left(\frac{r_0}{R}\right) - \ln R + \ln\left|r_0^2 - R^2\right|\right]. \tag{26}$$

As a check on this expression, E_{circle} depends only on r_0. Conservation of energy and Hamilton's equations confirm that the vortex moves on closed circular orbits with angular velocity (22) or (24).

5.1 Complex potential for a vortex outside an elliptical boundary

We start from the complex potential Eq. (23) and use the Joukowsky map to find

$$\begin{aligned} F_{\text{outside-ellipse}}(w;w_0) &= F_{\text{circle}}\left(\mathfrak{Z}(w);\mathfrak{Z}(w_0)\right) \\ &= \mathfrak{n}_0 \ln \mathfrak{Z}(w) + \ln\left[\mathfrak{Z}(w)-\mathfrak{Z}(w_0)\right] - \ln\left[\mathfrak{Z}(w)-\frac{(a+b)^2}{\mathfrak{Z}(w_0)^*}\right]. \end{aligned} \quad (29)$$

The real part is the stream function and the imaginary part is the phase function. Figure 1 uses these real functions to plot the stream lines and phase pattern for two cases: $\mathfrak{n}_0 = 0$ and $\mathfrak{n}_0 = 1$. These figures have all the expected features and verify that the proposed Joukowsky mapping from a circle to an ellipse is correct.

Majic [28] used elliptic coordinates to study the potential of a two-dimensional point charge outside an elliptical grounded conducting surface. The resulting real expression was an infinite series, in contrast to the real part of the complex potential in Eq. (29), which is a simple sum of three logarithms. Moreover, our formalism has the advantage of giving not only the streamlines, but also the phase plots. As shown below, it yields many other physical results such as the vortex dynamics and the vortex self energy $E_{\text{outside-ellipse}}$, all expressed ~~in closed form~~ explicitly in terms of well-known mathematical functions.

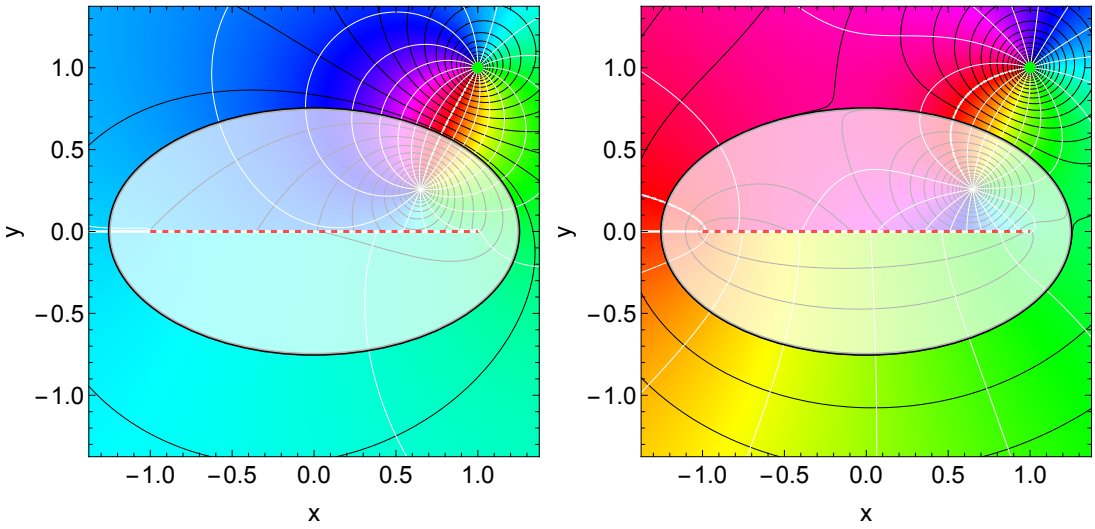

Figure 1: Real and imaginary parts of Eq. (29) giving streamlines (black lines) and phase (colour coding, and white lines) for a vortex outside of an ellipse (indicated respectively by the bright green dot and the black thick contour). The ellipse has aspect ratio $b/a = 0.6$, and its two foci are joined by the red dashed line. Left panel: $\mathfrak{n}_0 = 0$, meaning circulation $\mathfrak{n}_i = -1$ around the elliptical boundary. Right panel: $\mathfrak{n}_0 = 1$, meaning circulation $\mathfrak{n}_i = 0$ around the elliptical boundary.

5.2 Energy of a vortex outside an elliptical boundary

Equation (9) applies directly here, using Eq. (26) for E_z. For the circular boundary, the radial position is $r_0 = |z_0|$ with $R = a + b$ and $R_\infty = a_\infty$. The inverse transformation in Eq. (28) gives $d\mathfrak{Z}(w)/dw = \mathfrak{Z}(w)/\sqrt{w^2-1}$, so that $\sigma(w) = \ln \mathfrak{Z}(w) - \ln\left(w^2-1\right)/2$. In this way, we find

the compact result for the energy of a vortex at w_0 outside an elliptical boundary

$$E_{\text{outside-ellipse}} = \frac{\pi\hbar^2 n}{M}\left[\mathfrak{n}_0^2 \ln\left(\frac{a_\infty}{a+b}\right) - 2\mathfrak{n}_0 \ln\left(\frac{|\mathfrak{Z}(w_0)|}{a+b}\right) - \ln(a+b) + \ln\left(|\mathfrak{Z}(w_0)|^2 - (a+b)^2\right) + \frac{1}{2}\ln|w_0^2-1| - \ln|\mathfrak{Z}(w_0)|\right]. \tag{30}$$

Equipotential curves of this energy for $\mathfrak{n}_0 = 0$ are closed vortex orbits around the elliptical boundary, as shown in Fig. 2. To understand this figure, we consider a single vortex at a small distance $d \ll a$ outside the elliptical boundary. ~~The boundary condition on the tangential flow requires a single image vortex a distance $2d$ away, which dominates the complex potential. The corresponding energy diverges like $\ln 2d$ and the tangential velocity varies like $1/d$.~~ If d is much smaller than the local radius of curvature, then the boundary is effectively flat. In this case, the condition of tangential flow at the boundary requires an opposite-sign image at a distance d inside the boundary. The vortex and its effective image dominate the complex potential, which then approximates that of a vortex dipole with separation $2d$. The energy has a logarithmic dependence $\propto \ln(2d)$, and the translational velocity is $\propto 1/(2d)$ [5]. Considering the simple case $w_0 = a + d$ and Taylor expanding up to linear order in $d/a \ll 1$, one can see that the logarithmic behaviour of the energy arises from the first term in the second line of Eq. (30). Conservation of energy requires that d remains constant, so that the corresponding closed constant-energy curve follows the shape of the boundary. The increased density of contour lines near the boundary reflects the increasingly rapid precession near the elliptical surface, as expected from Hamilton's equations.

The situation is quite different for a vortex far from the boundary, as seen from Fig. 2, where such curves become circular. In the limit $|w_0| \gg 1$, in fact, $|\mathfrak{Z}(w_0)| \approx 2|w_0|$ and $\frac{1}{2}\ln|w_0^2 - 1| \approx \ln|w_0|$, so that the energy (30) reduces to Eq. (26) for a vortex outside a circular boundary.

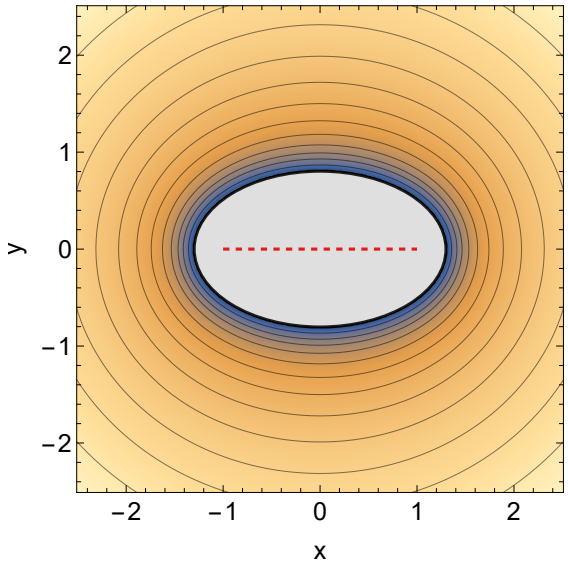

Figure 2: Contours of equal energy for a flow with $\mathfrak{n}_0 = 0$ around an ellipse with aspect ratio $b/a = 0.6$. The energy varies monotonically from large negative values (dark blue) to large positive ones (light orange).

Then, the velocity for a vortex at position w_0 inside the ellipse follows directly from Eq. (13) as:

$$i\dot{w}_0^* = \frac{\hbar}{2M}\left\{-\frac{w_0}{w_0^2-1}+\frac{i}{\sqrt{w_0^2-1}}\left[\frac{\vartheta_1'(i\ln\mathfrak{Z}_0,q)}{\vartheta_1(i\ln\mathfrak{Z}_0,q)}+\right.\right.$$
$$\left.\left.+\frac{\vartheta_1'\left(-\frac{i}{2}\ln\left(q\,|\mathfrak{Z}_0|^2\right),q\right)}{\vartheta_1\left(-\frac{i}{2}\ln\left(q\,|\mathfrak{Z}_0|^2\right),q\right)}-\frac{\vartheta_1'\left(-\frac{i}{2}\ln\left(q\frac{\mathfrak{Z}_0^*}{\mathfrak{Z}_0}\right),q\right)}{\vartheta_1\left(-\frac{i}{2}\ln\left(q\frac{\mathfrak{Z}_0^*}{\mathfrak{Z}_0}\right),q\right)}\right]\right\}. \tag{43}$$

We numerically integrated these complex dynamical equations for various initial conditions along the positive real axis, giving the closed trajectories shown in the right panel of Fig. 5. As proved in Sec. 2.2.1, these orbits are also contours of constant energy, and we checked that they indeed coincide with the curves shown in the left panel of Fig. 5. Note that these orbits differ greatly from the confocal ellipses in the right panel of Fig. 3. Instead they resemble nested self-similar ellipses, which is not surprising because the elliptical boundary is a quadrupolar distortion of a circle. Thus the closed trajectories for the elliptical boundary should resemble a set of nested circles with quadrupolar distortions.

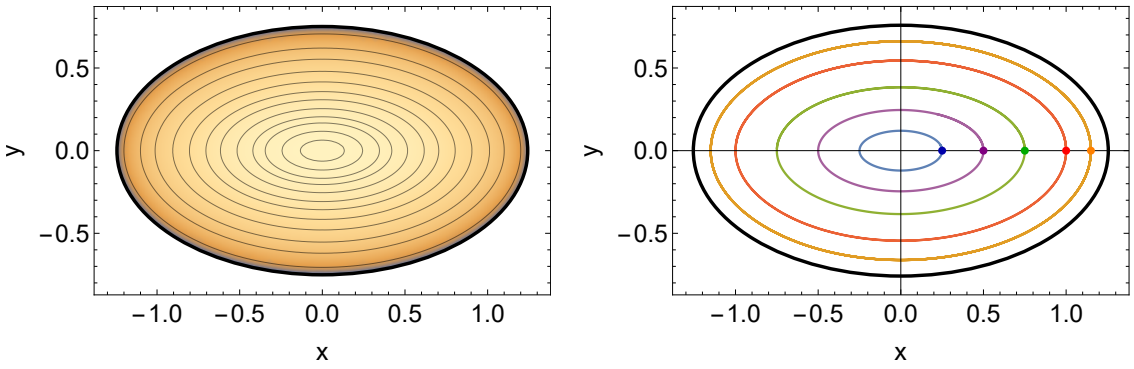

Figure 5: Left: constant-energy contours for a vortex inside an ellipse with aspect ratio $b/a = 0.6$. The thick black line denotes the outer boundary with $a = 5/4$ and $b = 3/4$. The vortex energy is negative and it decreases moving from the centre towards the boundaries. Right: trajectories of a single vortex inside the same elliptical boundary for various initial positions on the positive horizontal axis. Coloured dots denote the starting point of the different trajectories, which are obtained from numerical solution of the equations of motion (43).

In detail, however, the situation is more complicated. For a circular boundary, the rotational symmetry ensures conservation of angular momentum, so that all vortex trajectories are circles. In contrast, an elliptical boundary does not conserve angular momentum because the boundary is invariant only under a finite rotation by $\pm\pi$. If we use an angular Fourier expansion for the trajectory, only even harmonics can occur, and the nonlinear dynamical equations couple the various Fourier amplitudes. As a result, the orbits are not strictly ellipses. More quantitatively, for a given trajectory we extract the maximum value of the coordinates $(x_{\max}, y_{\max})$ and the period T. Figure 6 shows $(x_0/x_{\max})^2 + (y_0/y_{\max})^2$ evaluated along the five closed trajectories in the right frame of Fig. 5. The quantity $(x_0/x_{\max})^2 + (y_0/y_{\max})^2$ deviates from the value 1 that it would have for a pure ellipse, displaying a periodic, anharmonic dependence on the polar angle $\theta_0 \in [0, 2\pi]$. As follows from its definition, the maximum value of 1 is reached at positions $(\pm x_{\max}, 0)$ and $(0, \pm y_{\max})$. The minimum value and the corresponding deviation from 1 differ for each case, but it always remains small (less than 1%). Starting from the smallest trajectory (blue curve), the amplitude of the oscillation increases (purple and green), until it reaches its maximum for the trajectory with $x_{\max} = 1$ (red), which

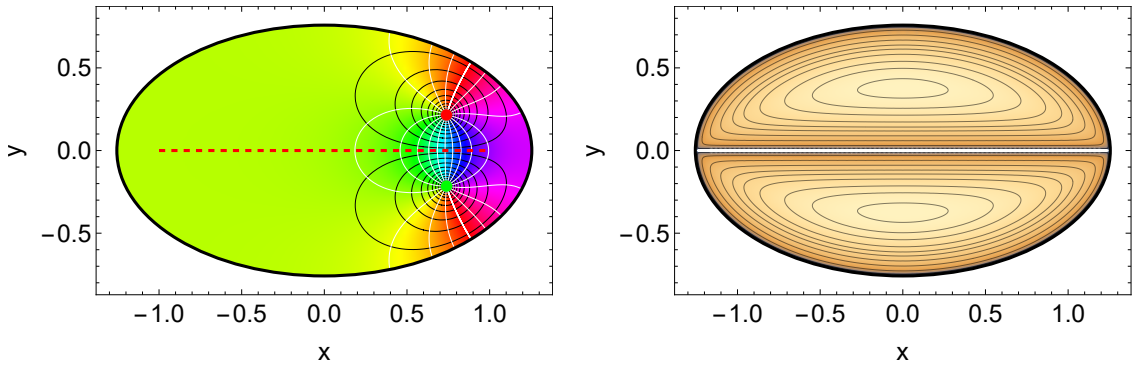

Figure 8: Left: streamlines (black lines) and phase (colour coding and white lines) associated with a symmetric vortex dipole inside the ellipse. This configuration consists of a positive vortex at position w_0 (red dot) and a negative one that is symmetric with respect to the focal line at position w_0^* (green dot). Right: constant-energy contours for the same symmetric vortex dipole. Colour coding is the same as in Fig. 5. The elliptical boundary has aspect ratio $b/a = 0.6$.

A plot of constant-energy contours is shown in the right panel of Fig. 8. The trajectories are qualitatively similar to the ones described by a vortex dipole inside a circular boundary, which have been experimentally observed in Ref. [32].

7 Conclusions and outlook

An earlier paper by one of us [18] studied the low-lying equilibrium states of rotating superfluid He-II in an elliptical cylinder, using real elliptic coordinates with infinite series for the resulting analytic solutions. Here, instead, we relied on complex variables and conformal maps that permit a unified description of general bounded and curved two-dimensional surfaces. Reference [30] developed this formalism to relate the energy of vortices on a complicated surface to the corresponding energy on a simple surface through the metric of the conformal map connecting them. Here we demonstrated that a similar derivation yields the dynamical equations of vortices on general two-dimensional surfaces with boundaries. We also verified that Hamilton's equations (based on the energy of the vortex) reproduce the vortex dynamics obtained with our complex formalism (based on conformal maps).

A circular boundary with radius R served as our model system because it is easy to derive the dynamics and energy of a vortex on either side of that boundary. To study vortex dynamics for an elliptical boundary, we used the Joukowsky map that takes a family of concentric circles into a family of confocal ellipses. This map worked well for a single vortex outside an elliptical boundary, giving the complex potential and the vortex orbits that are also the constant-energy curves.

The problem of a vortex inside an elliptical boundary became more intricate because the Joukowsky map introduced a branch cut along the line joining the two focal points of the ellipse. When combined with the inversion symmetry of the Joukowsky transformation, as seen in Fig. 3, the single circular boundary became an annulus with inner and outer boundaries at R^{-1} and R. The application of the Joukowsky map then provided the complex potential for a vortex inside an elliptical boundary, along with physical properties like the energy and trajectories. A straightforward generalization for multiple vortices allowed us to study the behaviour of a symmetric vortex dipole inside an elliptical boundary.

After this work was nearly completed, we belatedly discovered an earlier different confor-